

NACA TN 3911

File  
3042 03042  
d. n.f.

# ADVANCED RESEARCH DIVISION

## NATIONAL ADVISORY COMMITTEE FOR AERONAUTICS

TECHNICAL NOTE 3911

A METHOD FOR PREDICTING LIFT INCREMENTS DUE TO FLAP  
DEFLECTION AT LOW ANGLES OF ATTACK IN  
INCOMPRESSIBLE FLOW

By John G. Lowry and Edward C. Polhamus

Langley Aeronautical Laboratory  
Langley Field, Va.

CASE FILE  
COPY

Property Fairchild  
Engineering Library



Washington

January 1957

G  
NATIONAL ADVISORY COMMITTEE FOR AERONAUTICS

---

TECHNICAL NOTE 3911

---

A METHOD FOR PREDICTING LIFT INCREMENTS DUE TO FLAP  
DEFLECTION AT LOW ANGLES OF ATTACK IN  
INCOMPRESSIBLE FLOW

By John G. Lowry and Edward C. Polhamus

SUMMARY

A method is presented for estimating the lift due to flap deflection at low angles of attack in incompressible flow. In this method provision is made for the use of incremental section-lift data for estimating the effectiveness of high-lift flaps. The method is applicable to swept wings of any aspect ratio or taper ratio. The present method differs from other current methods mainly in its ease of application and its more general application. Also included is a simplified method of estimating the lift-curve slope throughout the subsonic speed range.

INTRODUCTION

Although several methods are currently available for estimating the effectiveness of flaps on wings of various plan forms (for example refs. 1 to 4), they are generally restricted to small flap deflections; and furthermore each method has certain reservations in its application. For example reference 1, which is a semiempirical approach, is limited to specific wing plan forms and flap-chord ratios within the range of experimental data used as well as to small flap deflections. In addition, both references 1 and 2 may require considerable manipulation to obtain values for a particular plan form.

The present method attempts to combine the various existing methods into a simple procedure that has more general applications than any one of them alone. Section lift data are used as a basis of the calculations, and this approach provides a means of estimating the increments of lift due to high-lift flaps at large deflections.

## SYMBOLS

A	aspect ratio
$a_0$	section lift-curve slope, per radian
b	wing span
$b_f$	flap span
$C_L$	three-dimensional lift coefficient
$\Delta C_L$	increment of three-dimensional lift coefficient due to flap deflection
$C_{L\alpha}$	three-dimensional lift-curve slope, per deg
$C_{L\delta} = \frac{\partial C_L}{\partial \delta}$ (constant $\alpha$ )	
c	wing chord
$c_f$	flap chord
$c_l$	two-dimensional section-lift coefficient
$\Delta c_l$	increment of section-lift coefficient due to flap deflection
$c_{l\alpha}$	section lift-curve slope, per deg
$K_b$	flap-span factor (ratio of partial-span-flap lift coefficient to full-span-flap lift coefficient), $\frac{(\Delta C_L) \text{ partial span}}{(\Delta C_L) \text{ full span}}$
$K_c$	flap-chord factor (ratio of three-dimensional flap-effectiveness parameter to two-dimensional flap-effectiveness parameter), $(\alpha_\delta)_{C_L} / (\alpha_\delta)_{c_l}$
M	Mach number
$\alpha$	angle of attack, deg
$(\alpha_\delta)_{C_L}$	three-dimensional flap-effectiveness parameter at constant lift

$(\alpha_{\delta})_{c_l}$  two-dimensional flap-effectiveness parameter at constant lift

$\delta$  flap deflection normal to hinge line, deg

$\delta'$  flap deflection streamwise,  $\tan \delta' = \tan \delta \cos \Lambda_h$ , deg

$\Lambda$  angle of sweep, deg

$\Lambda_h$  sweep of hinge line, deg

$\Lambda_c/2$  sweep of half-chord line, deg

$\Lambda_c/4$  sweep of quarter-chord line, deg

$\lambda$  taper ratio

Subscript:

eff effective

#### DEVELOPMENT OF METHOD

One reason for developing the present method is to provide a means of estimating the lift increment of high-lift flaps. The method is therefore based on the use of a section lift increment  $\Delta c_l$ , either theoretical or experimental. The basic concept used in the method is

$$\Delta C_L = C_{L\alpha} (\alpha_{\delta})_{c_L} \delta K_b \quad (1)$$

Since it is desired to use either a theoretical or an experimental value of  $\Delta c_l$  in the method and since

$$\Delta c_l = c_{l\alpha} (\alpha_{\delta})_{c_l} \delta$$

multiplying the right-hand side of equation (1) by  $\frac{\Delta c_l}{c_{l\alpha} (\alpha_{\delta})_{c_l} \delta}$   
gives

$$\Delta C_L = \Delta c_l \left( \frac{C_{L\alpha}}{c_{l\alpha}} \right) \left[ \frac{(\alpha_{\delta})_{c_L}}{(\alpha_{\delta})_{c_l}} \right] K_b \quad (2)$$

where  $\frac{C_{L\alpha}}{c_{l\alpha}}$  is the aerodynamic induction factor,  $\frac{(\alpha\delta)_{CL}}{(\alpha\delta)_{cl}}$  is the flap-chord factor  $K_c$ , and  $K_b$  is the flap-span factor,  $\frac{(\Delta C_L) \text{ partial span}}{(\Delta C_L) \text{ full span}}$

### Section-Lift-Coefficient Increments

The values of  $\Delta c_l$  used may be either two-dimensional experimental or theoretical values. For the purpose of this paper the section values are obtained in a streamwise direction; and flap deflection in the stream direction  $\delta'$  is used, since this plane is used for measuring the angle of attack. Several investigators have proposed that the section data should be referred normal to some sweep line since this concept would be in agreement with that used in the simple sweep theory. For airfoils in the range where the profile has a negligible effect on section characteristics (thin with small trailing-edge angle), the two methods give identical results for constant-percent-chord flaps on relatively untapered wings. For highly tapered wings the present method somewhat simplifies the difficulties, with regard to flap-chord ratios in the vicinity of the root and tip, that are encountered in the simple sweep theory. In view of this simplification and the fact that wings of current interest are relatively thin, the use of section data relative to the airplane center line is believed to be warranted. Since the values of  $\Delta c_l$  are the basis of the method, the final results will be only as accurate as the section data; therefore use of experimental data is advisable when such are available.

### Aerodynamic Induction Factor

The aerodynamic induction factor  $C_{L\alpha}/c_{l\alpha}$  depends upon the three-dimensional lift-curve slope  $C_{L\alpha}$ . A simplified method is presented in the appendix for estimating  $C_{L\alpha}$  which includes the effects of sweep, aspect ratio, and taper ratio. The appendix gives the following simple expression for the incompressible lift-curve slope (eq. (A6)):

$$C_{L\alpha} = \frac{\frac{a_0 A}{\pi} + \sqrt{\left(\frac{a_0}{\pi}\right)^2 + \left(\frac{A}{\cos \Lambda c/2}\right)^2}}{57.3}$$

Dividing both sides of this equation by  $c_{l\alpha}$  gives the following expression for the aerodynamic-induction factor:

$$\frac{C_{l\alpha}}{c_{l\alpha}} = \frac{A}{\frac{a_0}{\pi} + \sqrt{\left(\frac{a_0}{\pi}\right)^2 + \left(\frac{A}{\cos \Lambda_c/2}\right)^2}} \quad (3)$$

If both sides of equation (3) are divided by  $A$ , the expression  $\frac{1}{A} \left( \frac{C_{l\alpha}}{c_{l\alpha}} \right)$

is a unique function of  $\frac{A}{\cos \Lambda_c/2}$  for a given value of  $a_0$ , and the

relationship is shown in figure 1 for the case where  $a_0 = 2\pi$ . For estimations of  $\Delta C_L$  normally required, this curve should provide the value

of  $\frac{C_{l\alpha}}{c_{l\alpha}}$ ; if  $a_0$  differs appreciably from  $2\pi$ , the term should be com-

puted from equation (3) by using the most appropriate value of  $a_0$  available. The choice of  $\Lambda_c/2$  rather than the more commonly used  $\Lambda_c/4$  as the sweep angle for use in equation (3) is discussed in detail in the appendix. A nomograph for converting quarter-chord sweep angles to half-chord sweep angles is given in figure 2 for wings of various aspect ratio and taper ratio. An extension of the expression for  $C_{l\alpha}$  to account for compressibility is given in the appendix.

#### Flap-Span Effect

In order to apply the method to flaps other than full-span flaps, it is necessary to obtain a span-effectiveness factor  $K_b$  where

$$K_b = \frac{(\Delta C_L)_{\text{partial span}}}{(\Delta C_L)_{\text{full span}}}$$

An expression for the span-effectiveness factor for inboard flaps has been developed in reference 4 for wings having unswept trailing edges and streamwise tips (rectangular in the vicinity of the trailing edge). Equation (37) of reference 4 can be written as

$$K_b = \frac{2}{\pi} \left[ \frac{b_f}{b/2} \sqrt{1 - \left(\frac{b_f}{b/2}\right)^2} + \sin^{-1} \left( \frac{b_f}{b/2} \right) \right] \quad (4)$$

Examination of the results of references 5 and 6 and results obtained by using the 10-step method of reference 7 indicated that more accurate values can be obtained by using the empirical variations of  $K_b$  with  $\frac{b_f}{b/2}$  for the three taper ratios 0, 0.5, and 1.0 given in figure 3 than can be obtained from the single curve of equation (4). The following table gives the variation that can be expected when the curves of figure 3 are used.

Taper ratio	Aspect ratio	Variation in $K_b$
1.0	$1.5 < A < 12$	$\pm 0.02$
.5	$1.5 < A < 12$	$\pm 0.03$
0	$1.5 < A < 6$	$\pm 0.05$

If greater accuracy is required than is indicated by the table the span factor should be obtained by the methods of references 5 and 6.

For flaps other than inboard, the values are obtained by superposition of the flaps. This procedure is shown schematically in figure 4 for a midspan flap, and a similar method is used for outboard flaps.

#### Three-Dimensional Flap-Effectiveness Parameter

According to the assumptions of lifting-line theory, the section values of the flap-effectiveness parameter  $(\alpha_\delta)_{C_L}$  are independent of aspect-ratio effects. Because

$$(\alpha_\delta)_{C_L} = \frac{C_{L\delta}}{C_{L\alpha}}$$

and because, according to reference 8, the lifting-surface-theory correction to the lifting-line value is greater for  $C_{L\alpha}$  than for  $C_{L\delta}$ , a lifting-surface-theory correction to  $(\alpha_\delta)_{C_L}$  is necessary. The results of calculations for wings with a taper ratio of 1.0 and with flaps of constant  $c_f/c$  (ref. 4) were also used to obtain values of the factor  $K_c$  for wings of small aspect ratio. When the values from reference 4 and the limiting value for zero aspect ratio from reference 3 ( $(\alpha_\delta)_{C_L} = 1$  for all values of  $c_f/c$ ) were used, curves were established to provide the values of  $K_c$  as a function of aspect ratio for a range of values of  $(\alpha_\delta)_{C_L}$ . These curves are presented in figure 5, together with a plot showing the variation of  $(\alpha_\delta)_{C_L}$  with  $c_f/c$ . Because  $K_c$  is dependent

upon the type of chordwise loading, it might be expected to be more dependent upon  $c_f/c$  or upon the center of pressure than upon  $(\alpha_\delta)_{c_l}$ . However, the data available at the present time indicate a better correlation with  $(\alpha_\delta)_{c_l}$ .

Figure 6 presents a correlation of  $(\alpha_\delta)_{c_L}$  with values obtained from experimental  $C_{L\alpha}$  and  $C_{L\delta}$  data from reference 9 for wings having a constant-percent-chord flap with a value of  $(\alpha_\delta)_{c_l} = 0.60$ . The agreement between the estimated and the experimental variation with aspect ratio is very good.

When experimental values of  $\Delta c_l$  are used in order to estimate  $\Delta C_L$  for small deflections, the value of  $(\alpha_\delta)_{c_l}$  used in determining  $K_c$  can be obtained from experimental values or from the inset chart in figure 5. When large flap deflections are used and separation occurs over the flap, the values of  $(\alpha_\delta)_{c_l}$  can be obtained from

$$(\alpha_\delta)_{c_l} = \frac{57.3 \Delta c_l}{a_0 \delta} \quad (5)$$

If theoretical flap effectiveness is obtained by the use of boundary-layer control, the values of  $(\alpha_\delta)_{c_l}$  from the inset chart in figure 5 are used regardless of the value of  $\delta$ .

The effectiveness of flaps that have variable values of  $(\alpha_\delta)_{c_l}$  across the span is found by mechanical integration across the flap span of the following equation:

$$[(\alpha_\delta)_{c_l}]_{\text{eff}} = \frac{1}{K_b, \text{outboard} - K_b, \text{inboard}} \int_{K_b, \text{inboard}}^{K_b, \text{outboard}} (\alpha_\delta)_{c_l} dK_b \quad (6)$$

where the values of  $K_b$  are obtained from figure 3. When the values of  $(\alpha_\delta)_{c_l}$  are plotted against the values of  $K_b$  for all points along the flap span, then the area under the curve is equal to  $K_b [(\alpha_\delta)_{c_l}]_{\text{eff}}$ . For most configurations, however, an average value of  $(\alpha_\delta)_{c_l}$  will provide sufficient accuracy in the estimation of  $\Delta C_L$ .

For convenience, an experimental correlation of  $(\alpha\delta)_{c_l}$  for various flap chords is given in figure 7 for deflections of  $\pm 10^\circ$ . The experimental data were obtained from airfoils having trailing-edge angles of approximately  $10^\circ$  and includes both gap open and gap sealed conditions.

#### Experimental Verification

Since the usefulness of any method of estimating lift increments depends on the agreement obtained with actual results, the values of  $\Delta C_L$  obtained by the present method are compared with some experimental results in figure 8. The results of  $\Delta C_L$  are for the conditions of low speed ( $M < 0.4$ ) at  $\alpha = 0^\circ$ . The results at low flap deflections were obtained on unswept wings varying in aspect ratios from 1 to 6 and having flap-chord ratios varying from 0.10 to 0.40. The values of  $(\alpha\delta)_{c_l}$  used for the estimation were obtained from figure 7. A few comparisons are shown for double-slotted flaps deflected approximately  $60^\circ$  on both a swept wing and a delta wing. The section lift increments  $\Delta c_l$  were obtained from experimental two-dimensional data. It is apparent that the method, at least for the configuration shown in figure 8, is accurate for predicting the lift increment due to flap deflection.

#### CONCLUDING REMARKS

A simplified method is presented to provide for the estimation of the lift due to flap deflection on swept wings in incompressible flow from section data. A comparison of the experimental finite-span lift increments with those estimated by this method provides a satisfactory verification of the method.

Langley Aeronautical Laboratory,  
National Advisory Committee for Aeronautics,  
Langley Field, Va., October 10, 1956.

## APPENDIX

SIMPLIFIED METHOD OF ESTIMATING  $C_{L\alpha}$  THROUGHOUT  
THE SUBSONIC SPEED RANGE

The purpose of this appendix is to describe simple but accurate methods of estimating the effects of aspect ratio, sweep, taper ratio, and Mach number on the subsonic lift-curve slope.

Effect of Sweep, Aspect Ratio, and Mach Number

A very simple but accurate equation for the subsonic lift-curve slope is (for  $a_0 = 2\pi$ )

$$C_{L\alpha} = \frac{2\pi A}{2 + \sqrt{4 + \left(\frac{A}{\cos \Lambda}\right)^2 - (AM)^2}} \left( \frac{1}{57.3} \right) \quad (A1)$$

This equation, which is a modification of the Helmbold equation (ref. 10) to account for sweep and Mach number, was derived by the junior author, who originally presented it at a seminar (Ohio State University - Wright Patterson Air Force Base Graduate Center) in 1950. This expression is somewhat more accurate at low aspect ratios than the method presented in reference 11. An expression which gives identical results is derived in reference 12.

Equation (A1) can be derived simply by correcting the section lift-curve slope in Helmbold's equation (ref. 10) for the effect of sweep ( $a_0 \cos \Lambda$ ) and applying the well-known three-dimensional Prandtl-Glauert transformation. Correcting Helmbold's expression for the effect of sweep gives

$$(C_{L\alpha})_{M=0} = \frac{\frac{a_0 A}{\pi}}{\frac{a_0}{\pi} + \sqrt{\left(\frac{A}{\cos \Lambda}\right)^2 + \left(\frac{a_0}{\pi}\right)^2}} \left( \frac{1}{57.3} \right) \quad (A2)$$

Applying the three-dimensional Prandtl-Glauert transformation to account for compressibility gives

$$(C_{L\alpha})_M = \frac{a_0 A}{\frac{a_0}{\pi} + \sqrt{\frac{A^2(1 - M^2)}{\cos^2 \Lambda_M} + \left(\frac{a_0}{\pi}\right)^2}} \left(\frac{1}{57.3}\right) \quad (A3)$$

where  $\Lambda_M$  is defined as

$$\tan \Lambda_M = \frac{\tan \Lambda}{\sqrt{1 - M^2}}$$

By trigonometric substitution it can be shown that

$$\frac{A^2(1 - M^2)}{\cos^2 \Lambda_M} = A^2(1 - M^2) \left(1 + \frac{1}{\cos^2 \Lambda(1 - M^2)} - \frac{1}{1 - M^2}\right) = \left(\frac{A}{\cos \Lambda}\right)^2 - (AM)^2 \quad (A4)$$

and by substitution of equation (A4) in equation (A3)

$$(C_{L\alpha})_M = \frac{a_0 A}{\frac{a_0}{\pi} + \sqrt{\left(\frac{A}{\cos \Lambda}\right)^2 + \left(\frac{a_0}{\pi}\right)^2 - (AM)^2}} \left(\frac{1}{57.3}\right) \quad (A5)$$

This equation differs from that for the incompressible case (eq. (A2)) by only the term  $(AM)^2$ . The same result can be obtained by correcting the section lift-curve slope  $a_0$  in equation (A2) for compressibility by using the Mach number normal to the leading edge. Substituting

$$\frac{a_0}{\sqrt{1 - M^2 \cos^2 \Lambda}}$$

for  $a_0$  in equation (A2) and rearranging results in

$$(C_{L\alpha})_M = \frac{A}{\frac{1}{\pi} + \sqrt{\frac{A^2(1 - M^2 \cos^2 \Lambda)}{a_0^2 \cos^2 \Lambda} + \frac{1}{\pi^2}}} \left(\frac{1}{57.3}\right)$$

which reduces to equation (A5).

### Effect of Taper Ratio

It will be noted that no term for wing-taper-ratio effects appears in equation (A1). The effects of taper ratio, however, can be essentially eliminated if the half-chord line is used for the sweep reference line. This fact is illustrated in figure 9 where the incompressible lift-curve slope, as determined by the Weissinger 15-point method (refs. 5 and 6), is plotted as a function of the sweep of the quarter-chord line and the sweep of the half-chord line for various taper ratios. The results for an aspect ratio of 1.5 are presented in figure 9(a), and those for an aspect ratio of 3.0 are presented in figure 9(b). The results indicate that, when the usual procedure of referencing the sweep angle to the quarter-chord line is used, the effects of taper ratio on the lift-curve slope are rather large. However, when the half-chord line is used, the effect of taper is eliminated to a large extent. The fact that rather large effects of taper ratio occur for wings having the same sweep of the quarter-chord line (see left part of figs. 9(a) and 9(b)) can be explained to some extent at least by the reversibility theorem (ref. 13), which states that the lift-curve slope of a wing is the same in forward as in reversed flow. This theorem implies that if the sweep is referenced to a line other than the half-chord line, only the lift-curve slopes of the untapered wings ( $\lambda = 1.0$ ) will be symmetrical about zero sweep. It therefore is impossible for the lift-curve slopes of tapered wings to coincide with those of untapered wings throughout the sweep range, and at least an apparent taper-ratio effect must exist. The reversibility theorem itself, of course, does not exclude an actual taper-ratio effect; however, figure 9 shows that when the curves are made symmetrical by use of the half-chord line for the sweep reference, relatively little displacement due to taper ratio occurs. Also, in the modified lifting-line methods such as the Weissinger method, taper effects are dependent upon the sweep and the relative position of both the quarter-chord line (bound-vortex location) and the three-quarter-chord line (boundary-condition location). This fact suggests the possibility that wings having the same sweep of the intermediate or half-chord line might be less affected by taper than those having some other common sweep line.

### Accuracy of Method

The preceding results indicate that equation (A2) may be applicable to all plan forms, providing the sweep of the half-chord line is used. Use of  $\Lambda_c/2$  results in the following expression for the lift-curve slope:

$$(C_{I\alpha})_{M=0} = \frac{\frac{a_0 A}{\pi} + \sqrt{\left(\frac{a_0}{\pi}\right)^2 + \left(\frac{A}{\cos \Lambda_c/2}\right)^2}}{\frac{a_0 A}{\pi}} \left( \frac{1}{57.3} \right) \quad (A6)$$

Dividing both sides by  $A$  and letting  $a_0$  equal  $2\pi$  gives the following expression:

$$\frac{(C_L \alpha)_{M=0}}{A} = \frac{2\pi}{2 + \sqrt{4 + \left(\frac{A}{\cos \Lambda_c/2}\right)^2}} \left( \frac{1}{57.3} \right) \quad (A7)$$

which indicates that  $\frac{C_L \alpha}{A}$  is a unique function of  $\frac{A}{\cos \Lambda_c/2}$ . In order that the accuracy of the method may be evaluated, equation (A7) is compared with available lifting-surface solutions (refs. 14 to 18) in figure 10. The Swanson method used for the  $60^\circ$  sweptback elliptical wing is described in reference 8. The lifting-surface solutions presented are probably the most accurate solutions available, and it will be noted that they cover a wide range of plan forms. The fact, therefore, that the lifting-surface solutions are in excellent agreement with equa-

tion (A7) appears to indicate both that  $\frac{C_L \alpha}{A}$  is, for all practical purposes, a unique function of  $\frac{A}{\cos \Lambda_c/2}$  and that equation (A7) is sufficiently accurate.

### Design Charts

For the convenient determination of the lift-curve slope, some design charts are presented. Figure 11 presents the variation of

$\frac{C_L \alpha}{A}$  with  $\frac{A}{\cos \Lambda_c/2}$  for incompressible flow. For the convenient correction of these results for the effect of Mach number, correction factors are presented in figure 12 as a function of the half-chord sweep for various aspect ratios at Mach numbers of 0.40, 0.60, 0.80, 0.90, and 0.95. Since sweep angles are quite often referred to the quarter-chord line, a nomograph for converting from quarter-chord sweeps to half-chord sweeps is presented in figure 2.

## REFERENCES

1. Lowry, John G., and Schneiter, Leslie E.: Estimation of Effectiveness of Flap-Type Controls on Sweptback Wings. NACA TN 1674, 1948.
2. DeYoung, John: Theoretical Symmetric Span Loading Due to Flap Deflection for Wings of Arbitrary Plan Form at Subsonic Speeds. NACA Rep. 1071, 1952. (Supersedes NACA TN 2278.)
3. DeYoung, John: Spanwise Loading for Wings and Control Surfaces of Low Aspect Ratio. NACA TN 2011, 1950.
4. Stone, H. N.: Aerodynamic Characteristics of Low-Aspect-Ratio Wings With Various Flaps at Subsonic Speeds. Rep. No. AF-743-A-2 (Contract No. AF 33(038)-17397), Cornell Aero. Lab., Inc., Jan. 1952.
5. Diederich, Franklin W., and Zlotnick, Martin: Calculated Spanwise Lift Distributions, Influence Functions, and Influence Coefficients for Unswept Wings in Subsonic Flow. NACA Rep. 1228, 1955. (Supersedes NACA TN 3014.)
6. Diederich, Franklin W., and Zlotnick, Martin: Calculated Spanwise Lift Distributions and Aerodynamic Influence Coefficients for Swept Wings in Subsonic Flow. NACA TN 3476, 1955.
7. Campbell, George S.: A Finite-Step Method for the Calculation of Span Loadings of Unusual Plan Forms. NACA RM L50L13, 1951.
8. Swanson, Robert S., and Crandall, Stewart M.: Lifting-Surface-Theory Aspect-Ratio Corrections to the Lift and Hinge-Moment Parameters for Full-Span Elevators on Horizontal Tail Surfaces. NACA Rep. 911, 1948. (Supersedes NACA TN 1175.)
9. Dods, Jules B., Jr., and Tinling, Bruce E.: Summary of Results of a Wind-Tunnel Investigation of Nine Related Horizontal Tails. NACA TN 3497, 1955.
10. Helmbold, H. B.: Der unverwundene Ellipsenflügel als tragende Fläche. Jahrb. 1942 der Deutschen Luftfahrtforschung, R. Oldenbourg (Munich), pp. I 111 - I 113.
11. Polhamus, Edward C.: A Simple Method of Estimating the Subsonic Lift and Damping in Roll of Sweptback Wings. NACA TN 1862, 1949.
12. Diederich, Franklin W.: A Plan-Form Parameter for Correlating Certain Aerodynamic Characteristics of Swept Wings. NACA TN 2335, 1951.

13. Brown, Clinton E.: The Reversibility Theorem for Thin Airfoils in Subsonic and Supersonic Flow. NACA Rep. 986, 1950. (Supersedes NACA TN 1944.)
14. Krienes, Klaus: The Elliptic Wing Based on the Potential Theory. NACA TM 971, 1941.
15. Falkner, V. M. (With Appendix by Doris Lehrian): Calculated Loadings Due to Incidence of a Number of Straight and Swept-Back Wings. R. & M. No. 2596, British A.R.C., June 1948.
16. Dickson, R.: Comparison of Two Methods of Calculating Aerodynamic Loading on an Aerofoil With Large Sweepback and Small Aspect Ratio. R. & M. No. 2353, British A.R.C., June 1946.
17. Schneider, William C.: A Comparison of the Spanwise Loading Calculated by Various Methods With Experimental Loadings Obtained on a  $45^{\circ}$  Sweptback Wing of Aspect Ratio 8.02 at a Reynolds Number of  $4.0 \times 10^6$ . NACA Rep. 1208, 1954. (Supersedes NACA RM L51G30.)
18. Jones, Robert T.: Properties of Low-Aspect-Ratio Pointed Wings at Speeds Below and Above the Speed of Sound. NACA Rep. 835, 1946. (Supersedes NACA TN 1032.)

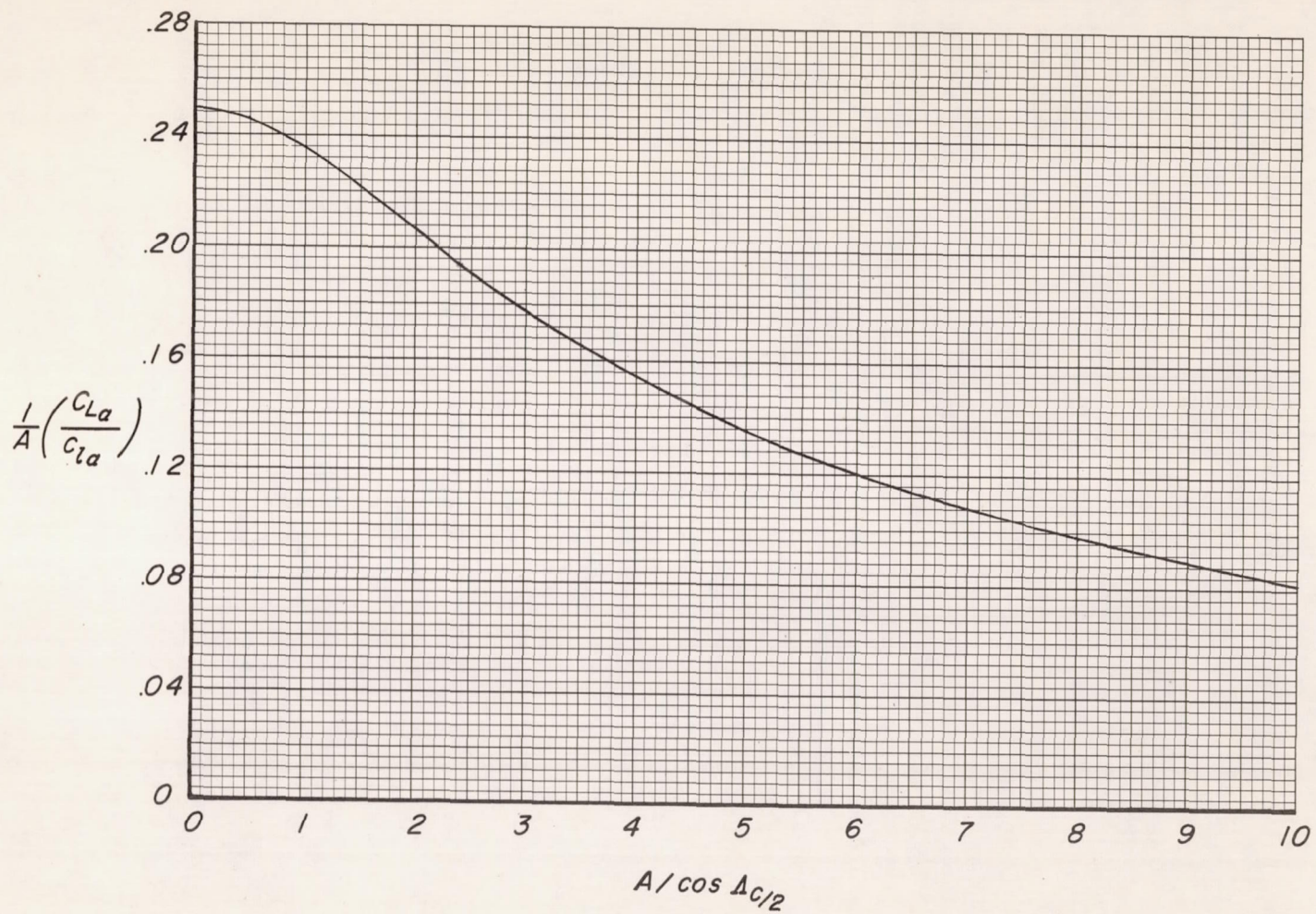


Figure 1.- Variation of aerodynamic induction factor  $\frac{1}{A} \left( \frac{C_{L\alpha}}{C_{l\alpha}} \right)$  with  $\frac{A}{\cos \Lambda_{c/2}}$ .  $a_0 = 2\pi$ ;  $M = 0$ .

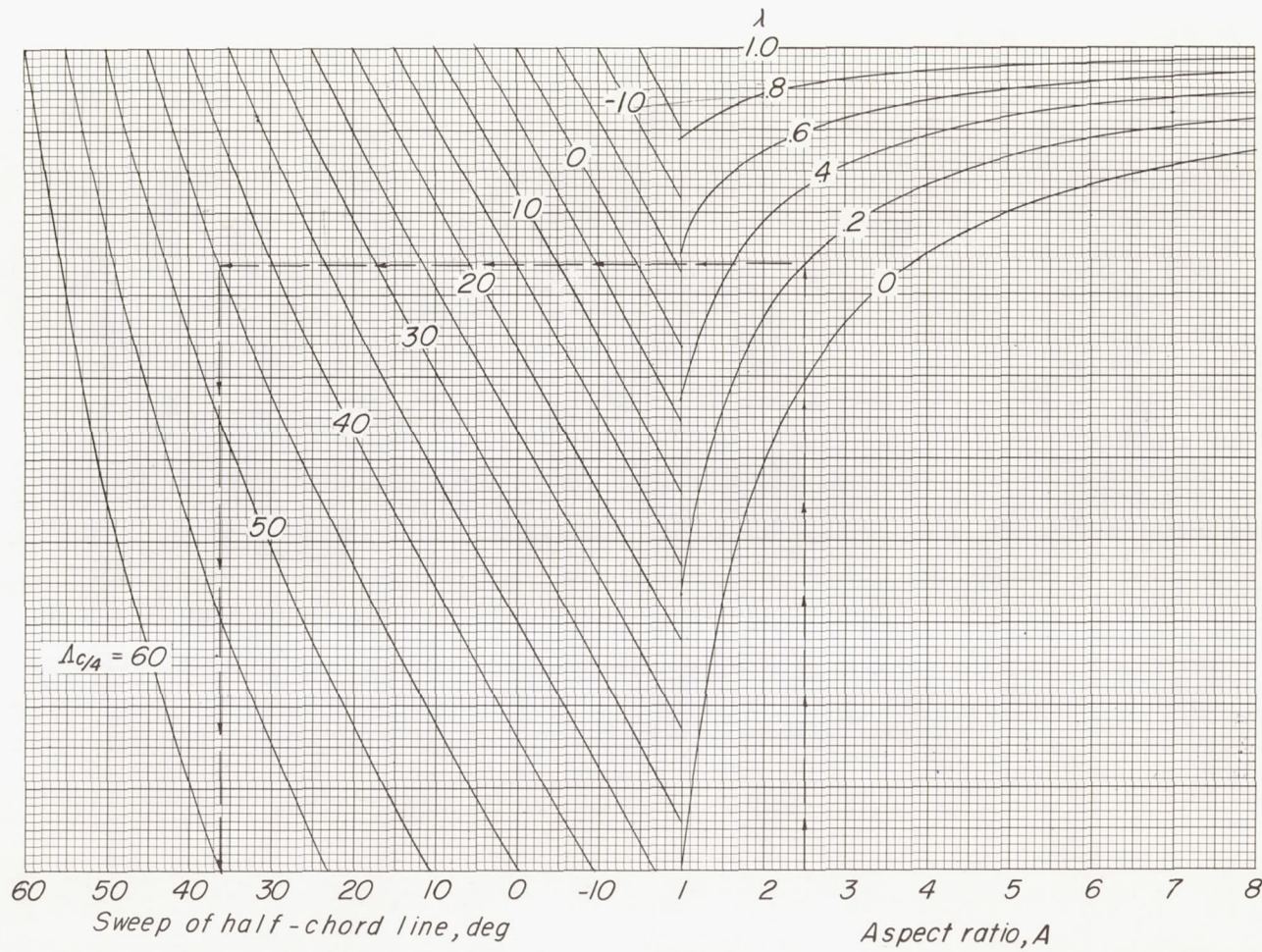


Figure 2.- Nomograph for converting quarter-chord sweep angles to half-chord sweep angles.

$$\tan \Lambda_c/2 = \tan \Lambda_{c/4} - \frac{1}{A} \left( \frac{1 - \lambda}{1 + \lambda} \right).$$

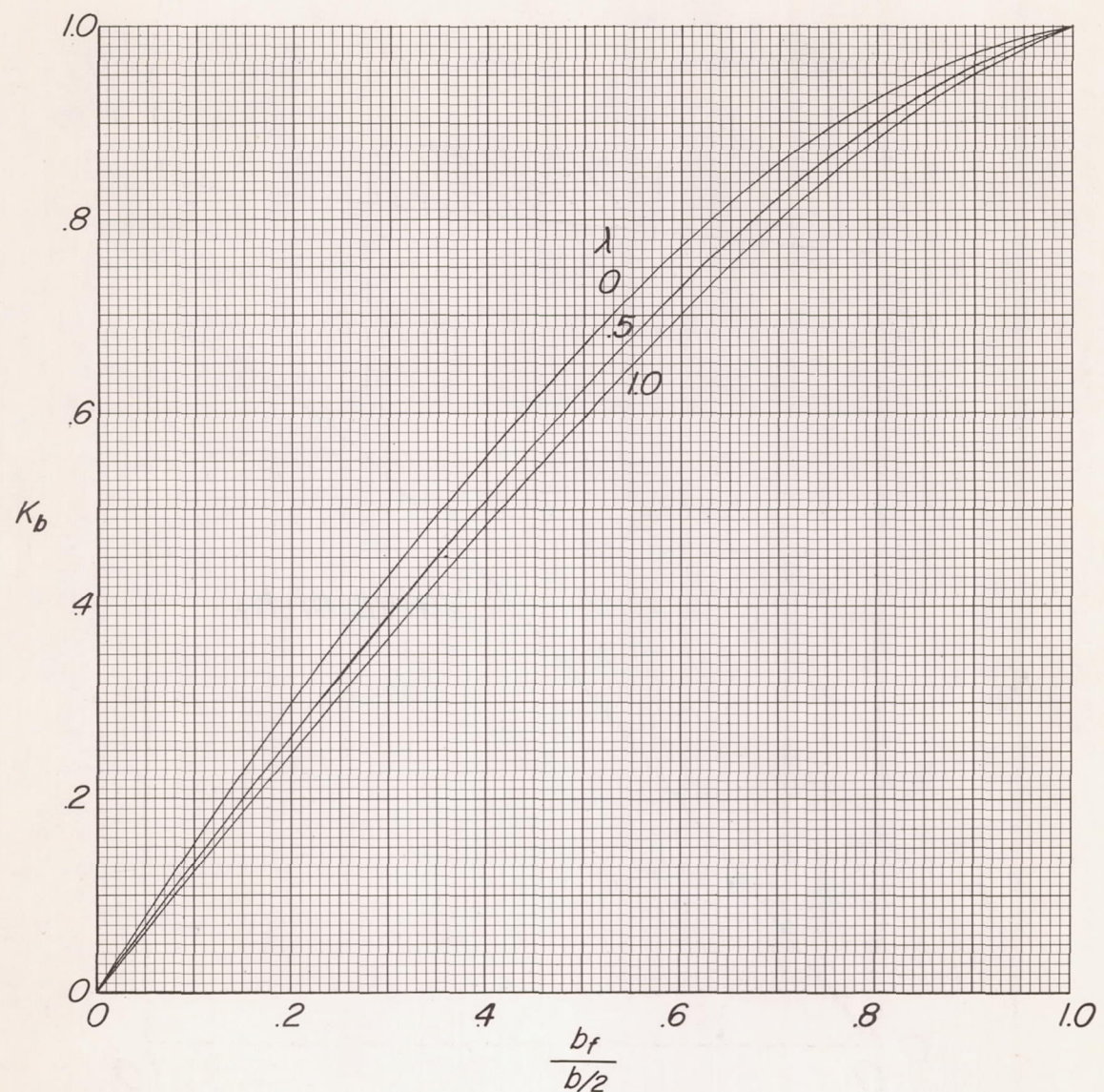


Figure 3.- Variation of span factor  $K_b$  with flap span for inboard flaps.

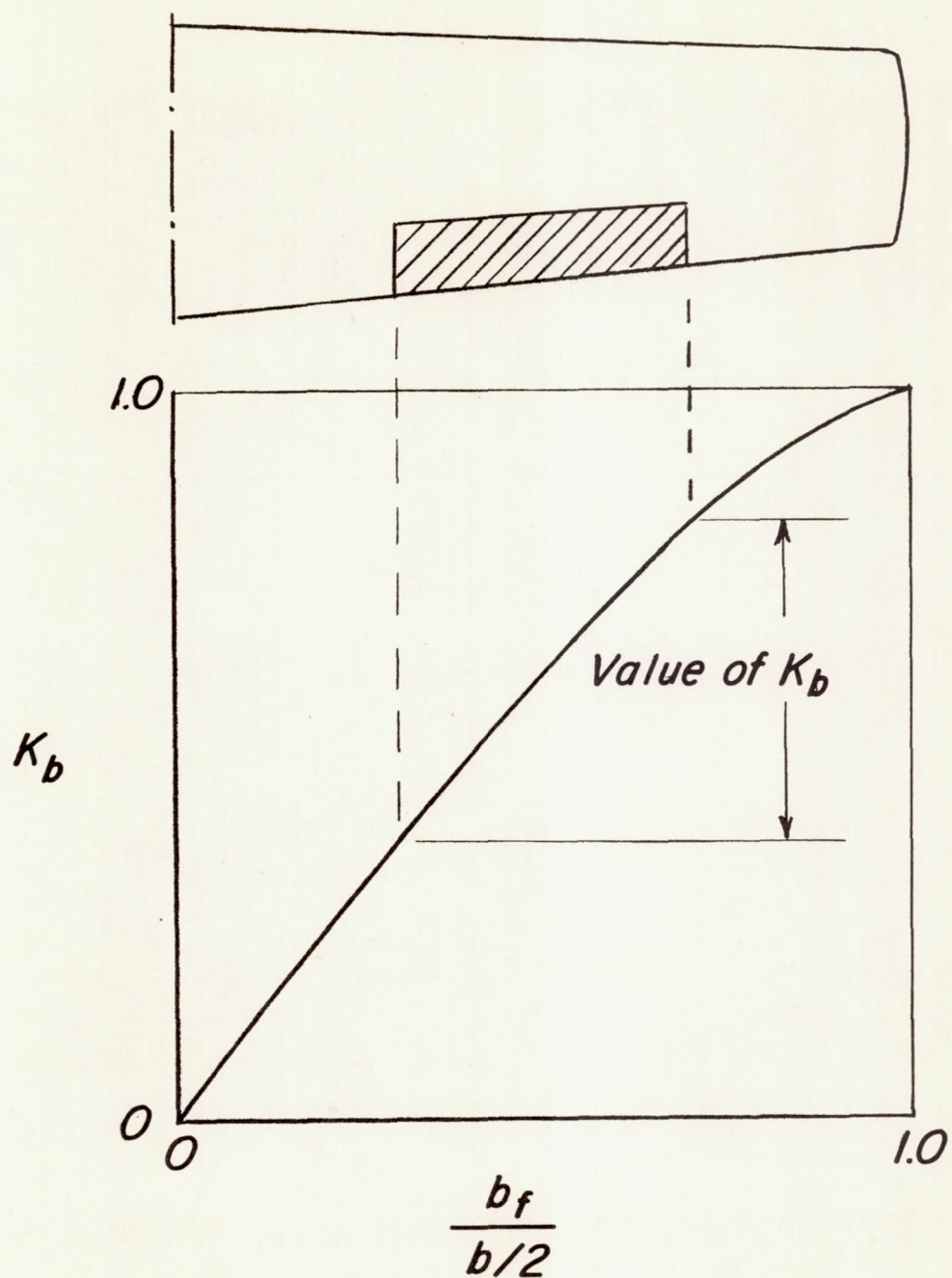


Figure 4.- Span factor for flaps other than inboard flaps.

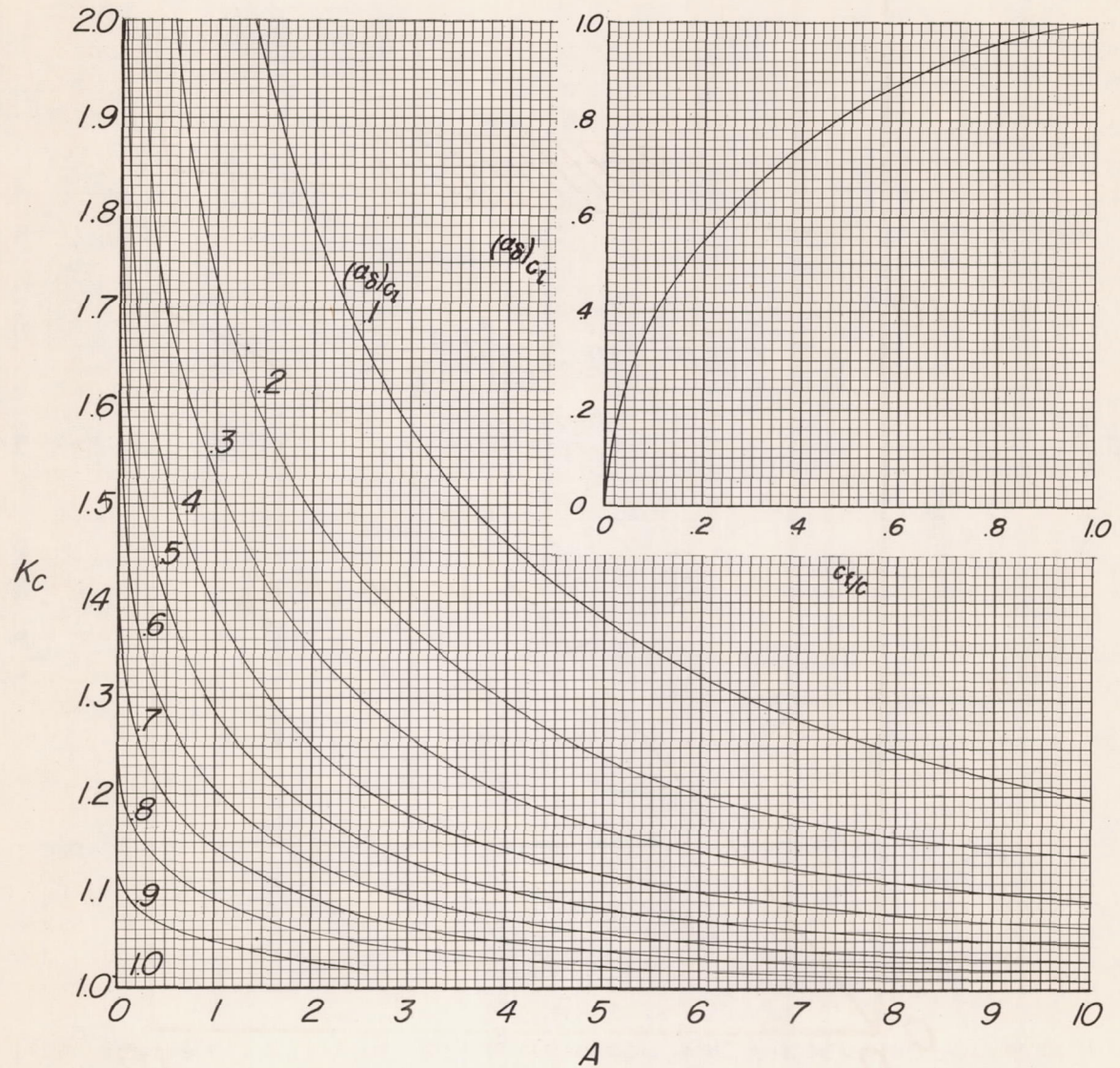


Figure 5.- Variation of flap-chord factor with  $(\alpha_\delta)_{c_l}$  and aspect ratio.

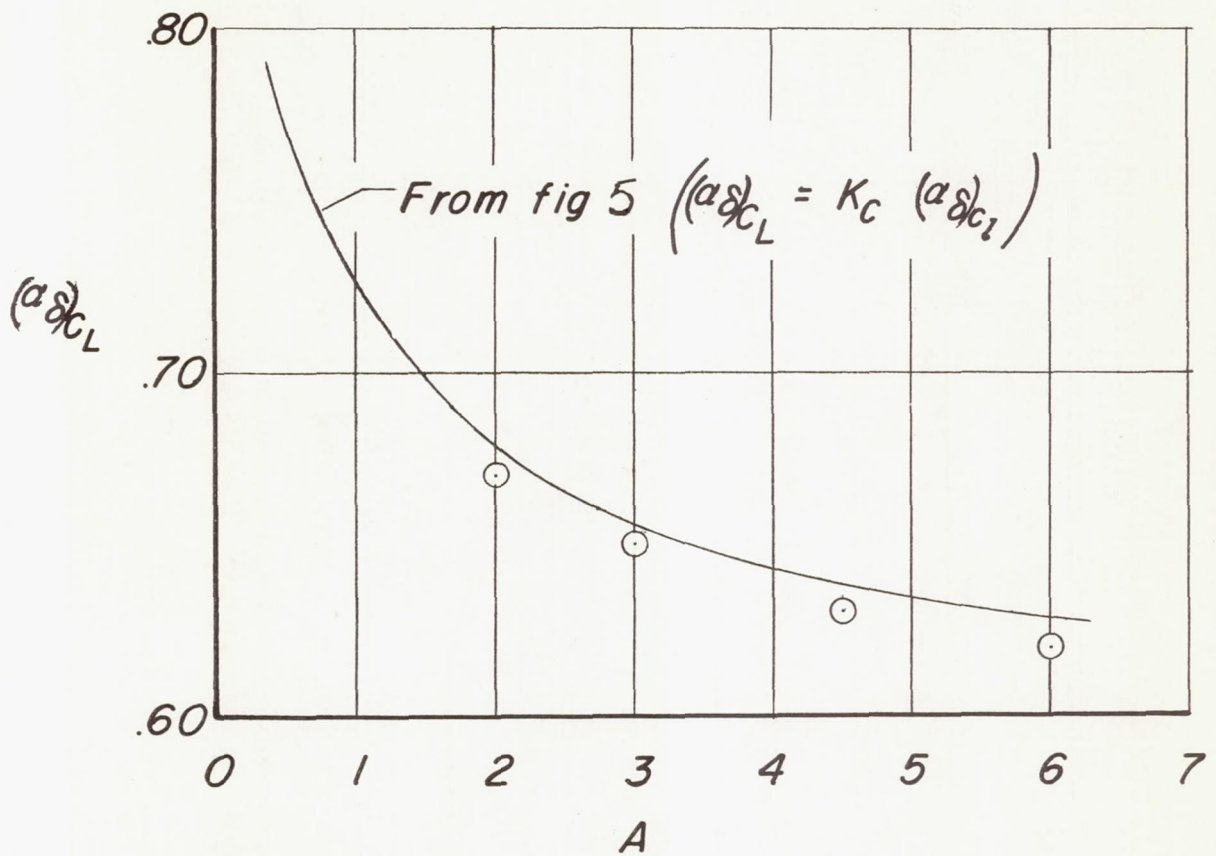


Figure 6.- Comparison of estimated values of  $(\alpha_{\delta})_{C_L}$  with experimental values of reference 9.  $(\alpha_{\delta})_{C_L} = 0.60.$

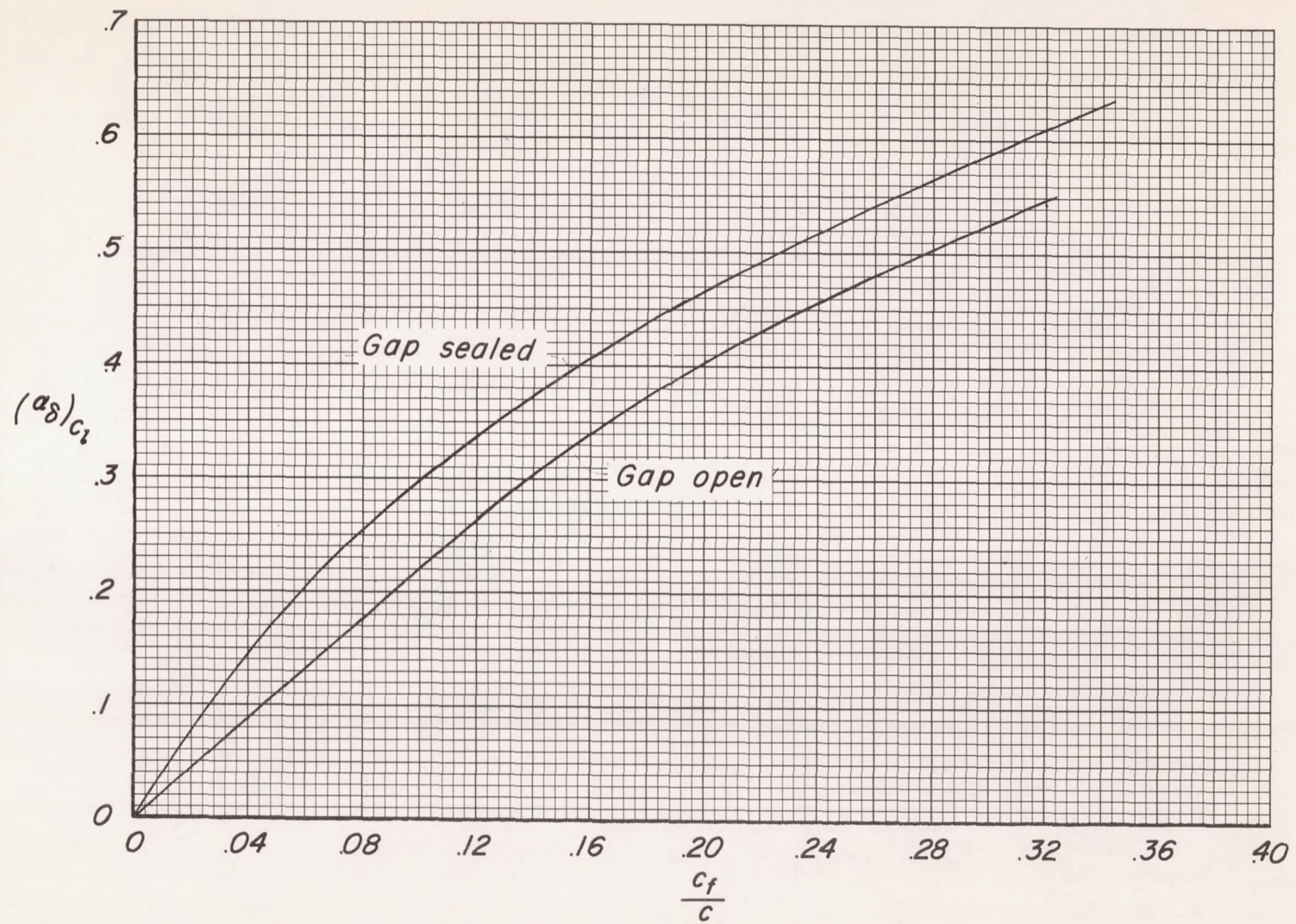


Figure 7.- Variation of flap-effectiveness parameter with control-chord ratio. Average trailing-edge angle approximately  $10^\circ$ ;  $M \leq 0.2$ ; flap deflection,  $\pm 10^\circ$ .

	$\delta_f$	$A c_{l_2}$	$\lambda$	$A$
○ Plain flap	10°	0	1	1 to 6
□ Double-slotted flap	60°	40°	.41	3.7
△ Double-slotted flap	60°	41°	0	2.31

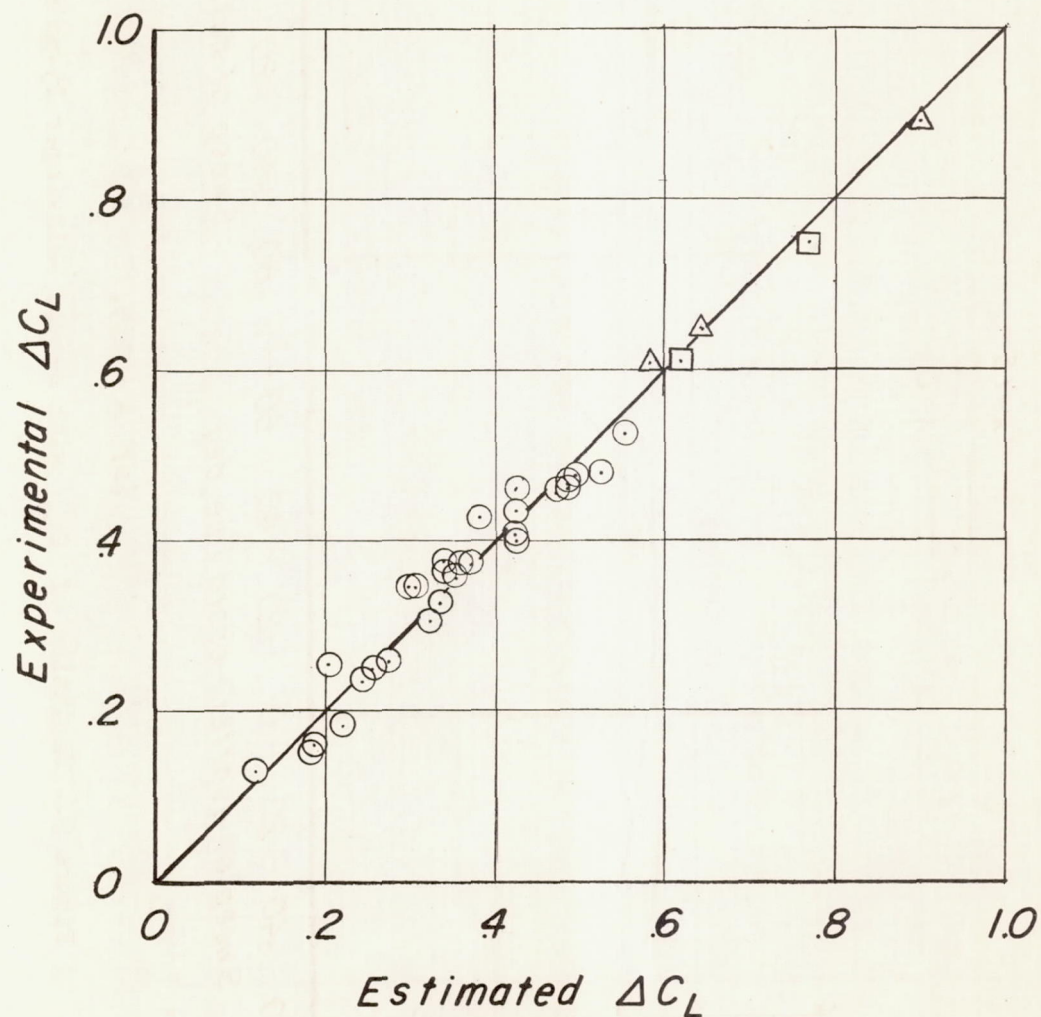


Figure 8.- Correlation of experimental and estimated values of  $\Delta C_L$ .  
 $\alpha = 0^\circ$ ;  $M < 0.4$ .

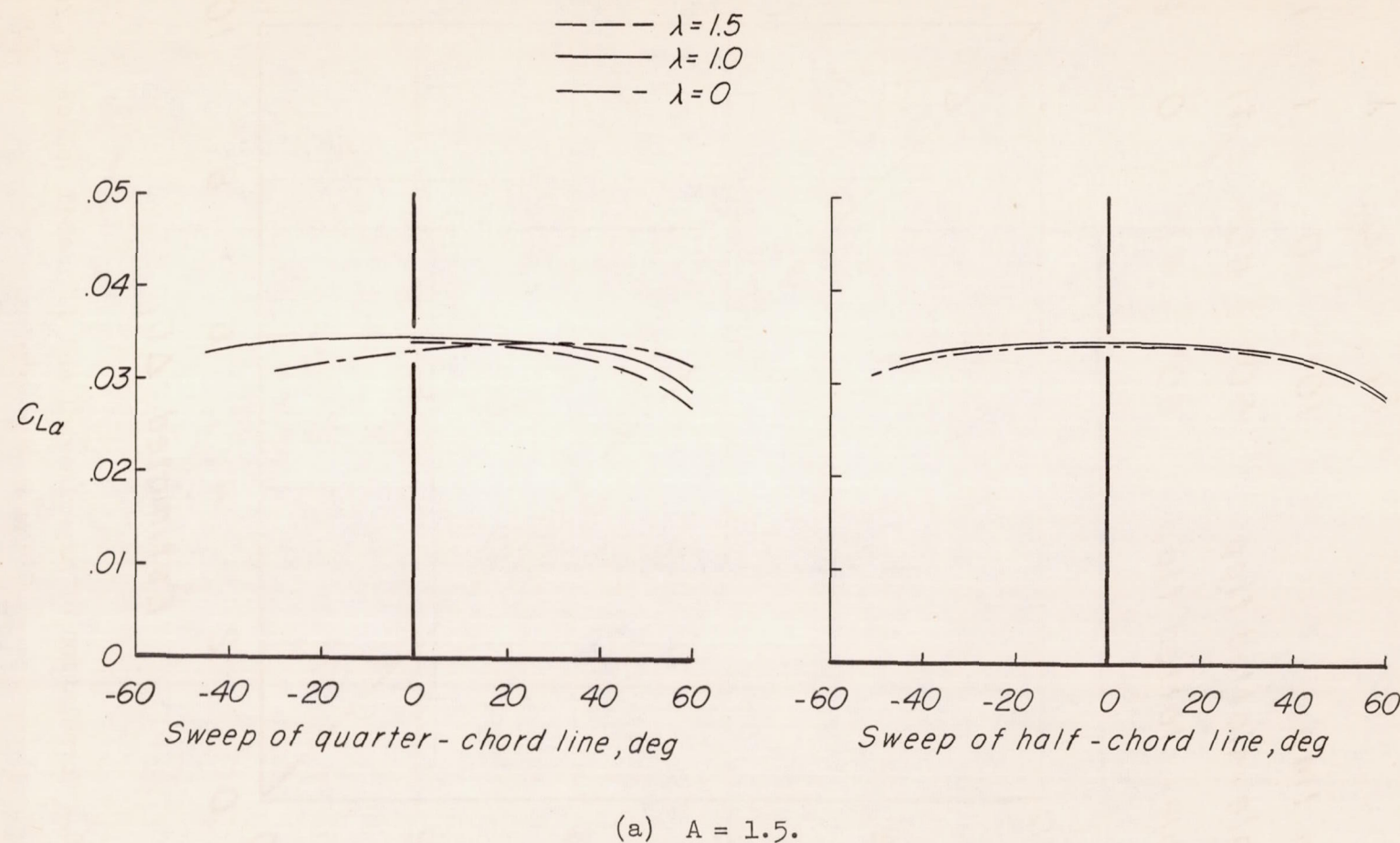


Figure 9.- Variation of  $C_{L\alpha}$  with sweep; Weissinger 15-point method.

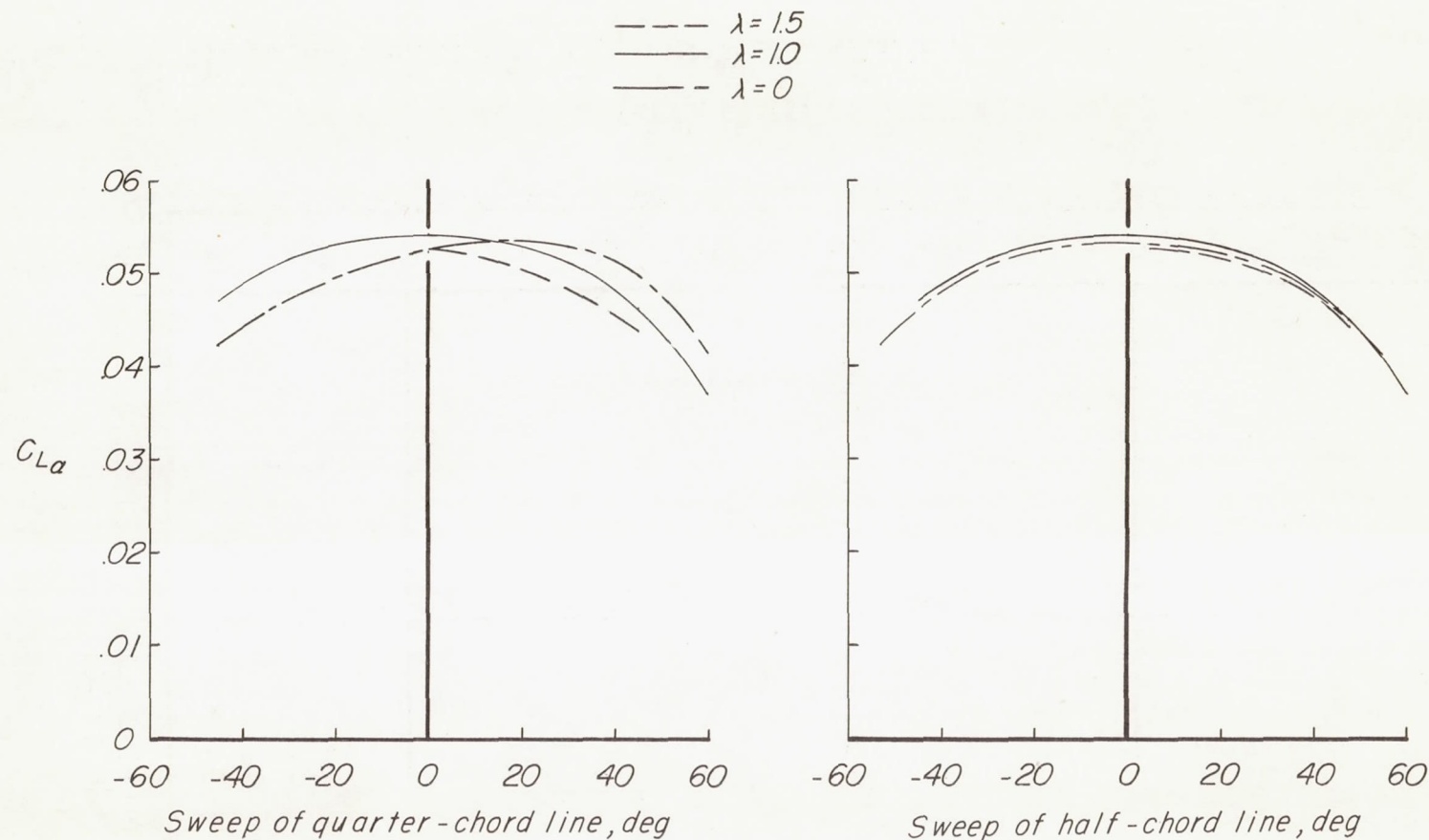
(b)  $A = 3.0.$ 

Figure 9.- Concluded.

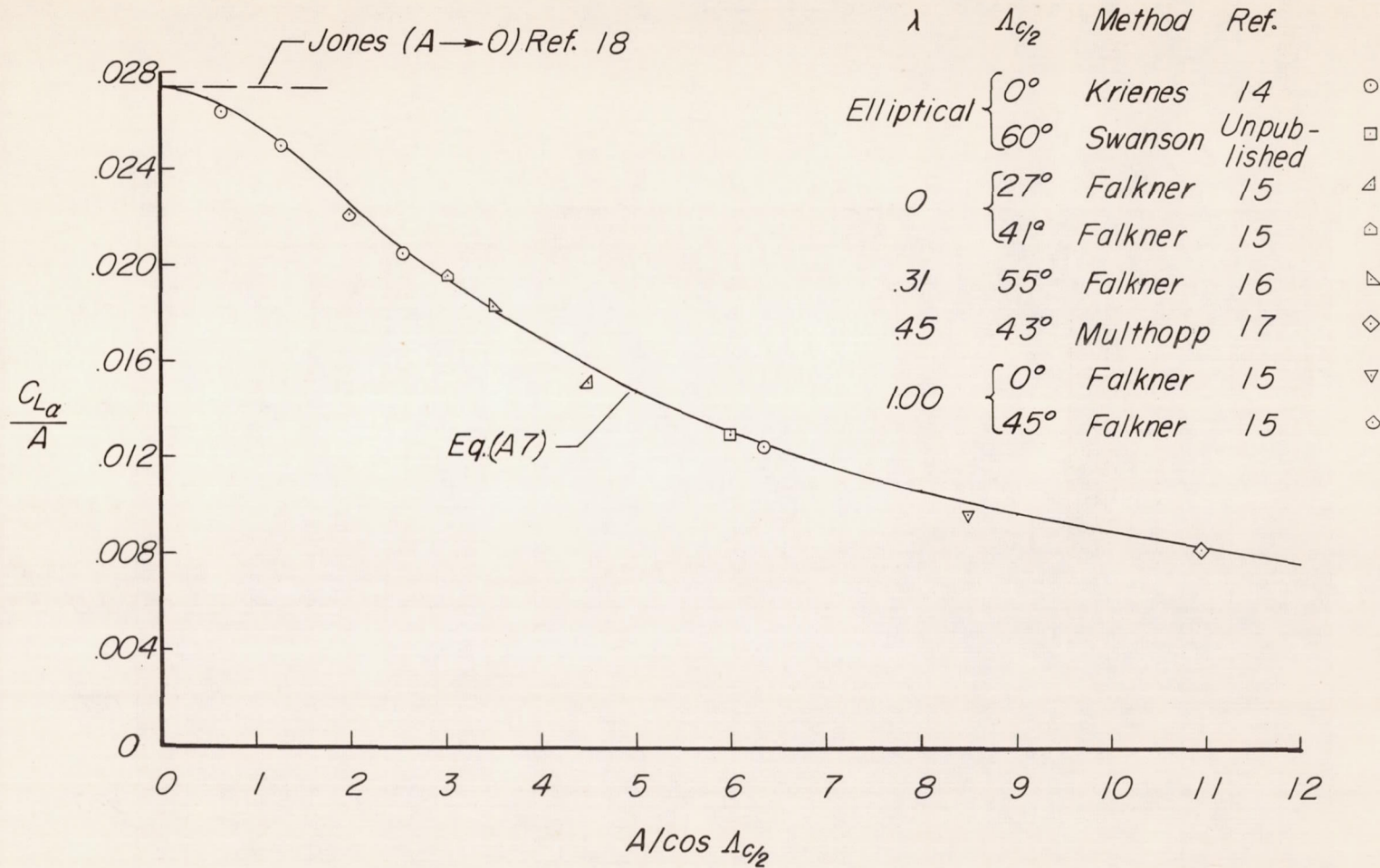


Figure 10.- Variation of  $\frac{C_{L\alpha}}{A}$  with  $\frac{A}{\cos \Lambda_{c/2}}$  as determined by several methods.  $a_0 = 2\pi$ ;  $M = 0$ .

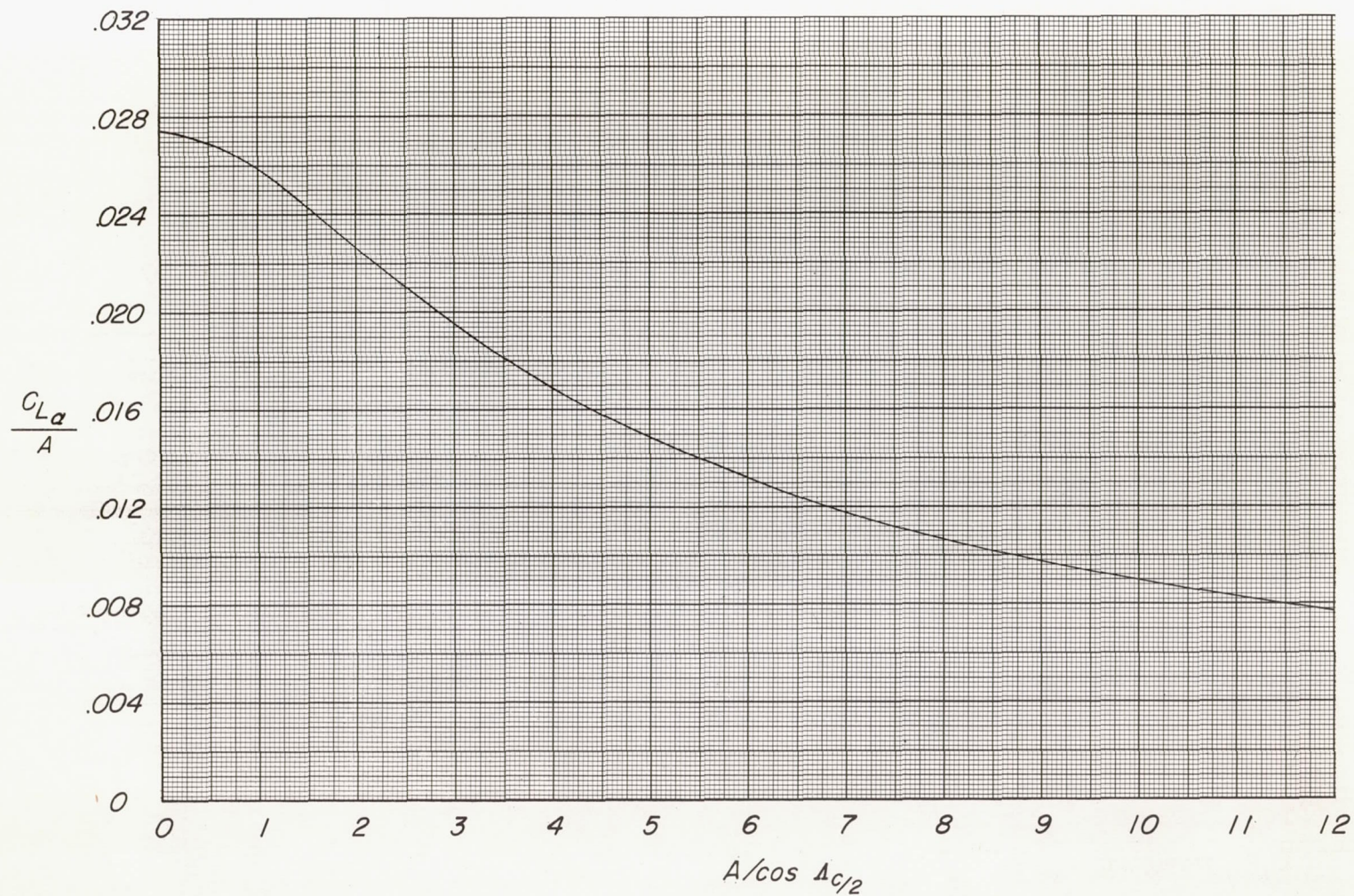


Figure 11.- Variation of  $\frac{C_{L\alpha}}{A}$  with  $\frac{A}{\cos \Lambda_C/2}$  in incompressible flow.

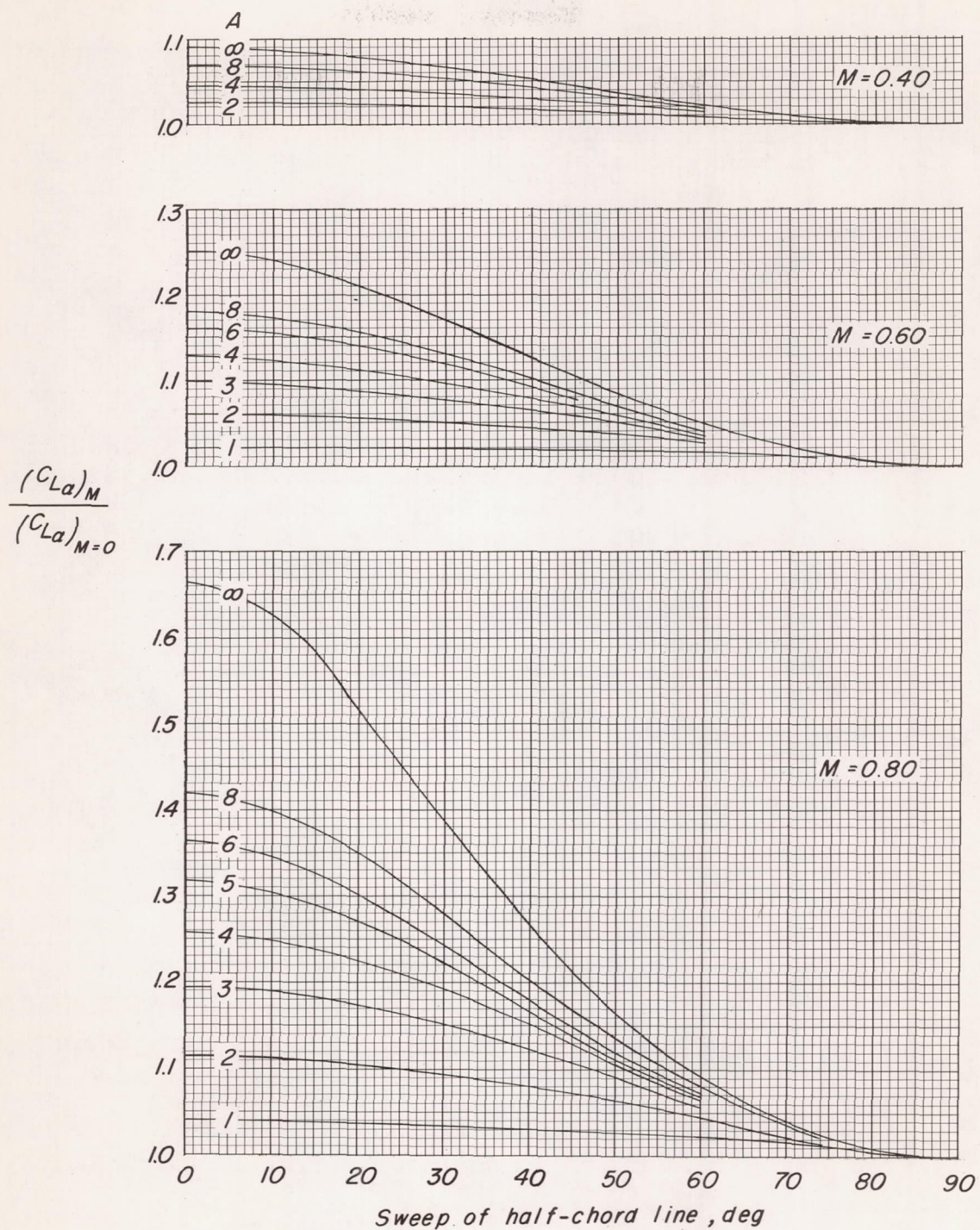


Figure 12.- Ratio of compressible to incompressible lift-curve slopes for subsonic speeds.

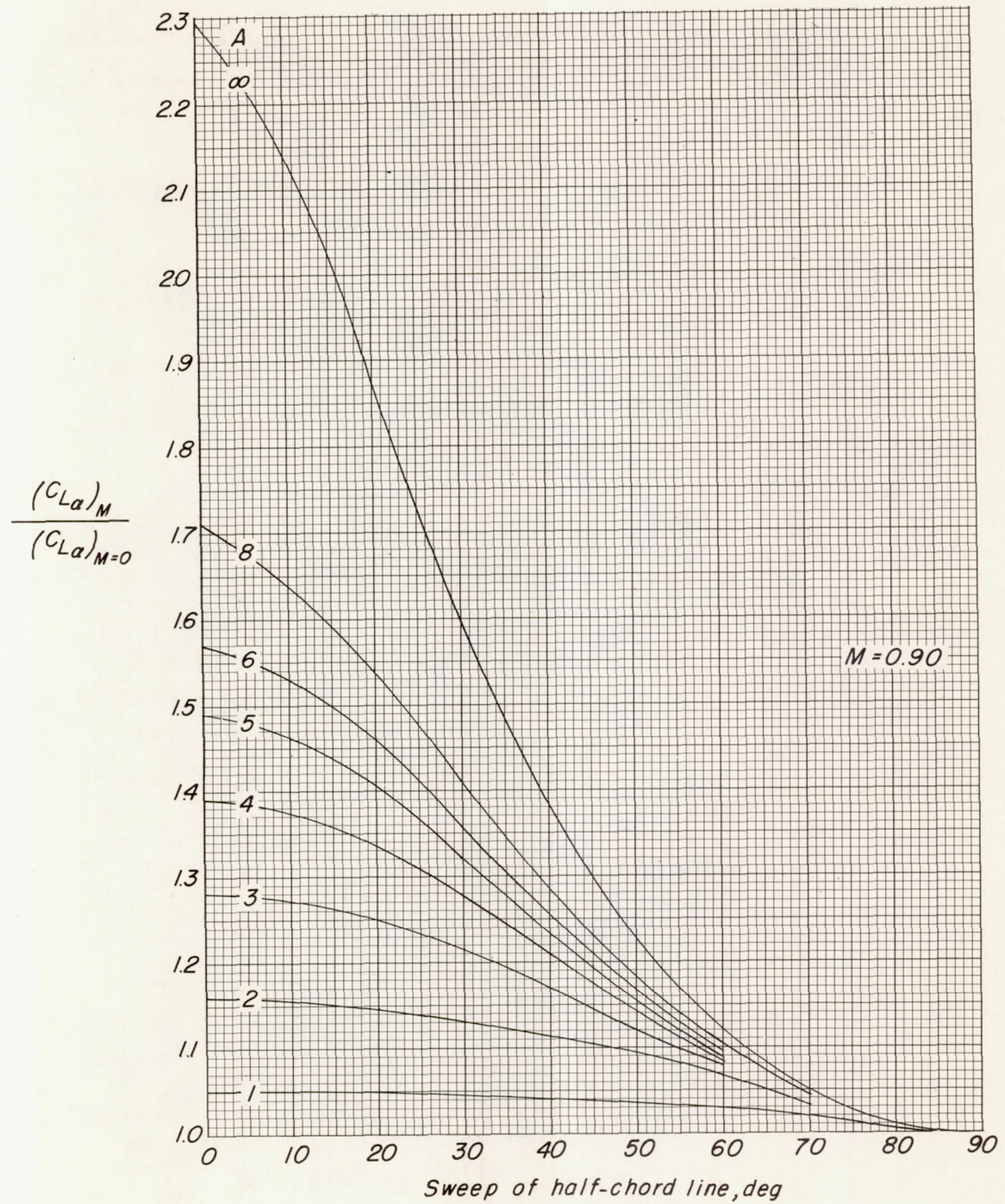


Figure 12.- Continued.

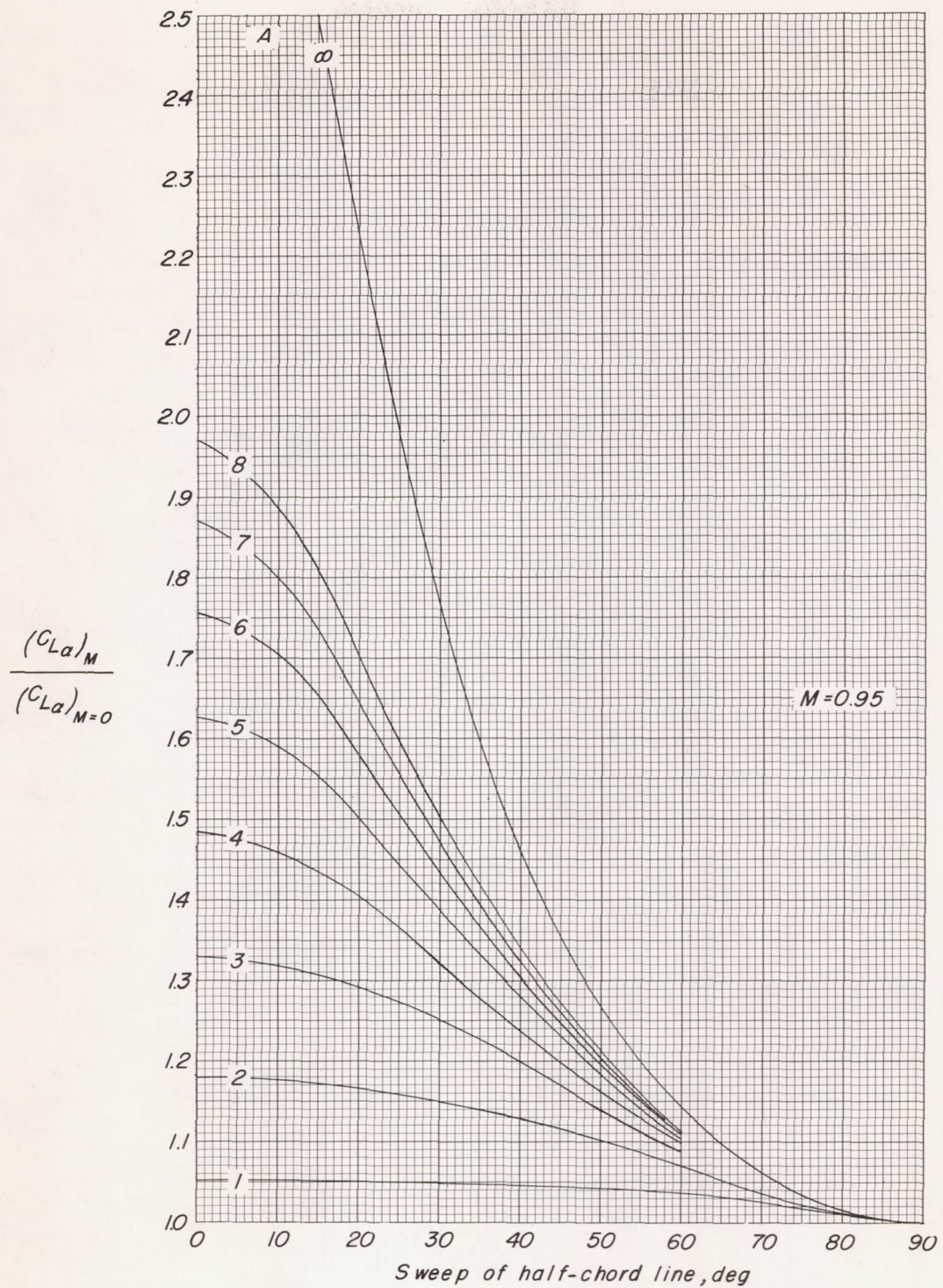


Figure 12.- Concluded.